JOURNAL OF MATERIALS SCIENCE 32 (1997) 1297–1304

Interfacial polycondensation of nylon-6,6 at the glass fibre surface and its effect on fibre–matrix adhesion

H. SALEHI-MOBARAKEH, J. BRISSON, A. AIT-KADI*†
*Department of Chemistry, and *Department of Chemical Engineering, Centre de Recherche en Sciences et Ingénierie des Macromolécules (CERSIM), Faculté des sciences et de génie, Université Laval, Québec, Canada G1K 7P4*

The surface of glass fibres was modified using chemical treatments to improve fibre–matrix interface properties. Interfacial polycondensation was performed with the fibre acting as the interface, and nylon-6,6 chains were grafted on the free hydroxyl groups located at the fibre surface. Grafted nylon was observed through the scanning electron microscope. The effect of the treatment on the fibre-matrix adhesion was investigated by measuring the interfacial shear strength in fragmentation micromechanical tests. The two-parameter Weibull distribution was used to analyse the experimental results. Polarized optical microscopy showed the existence of a transcrystalline layer in treated samples, indicating better fibre wettability by the matrix. Scanning electron microscopy confirmed the presence of an excellent bonding between fibre and matrix in treated samples, whereas in untreated samples, fibre pull-out was predominant, indicating poorer fibre–matrix adhesion.

1. Introduction

Fibre–matrix adhesion is an essential controlling factor for mechanical properties of composites. The ability of the interface to transfer a load from the matrix to fibres depends on physicochemical properties of both fibres and matrix. Poor bonding at the interface causes interfacial debonding and failure of the composites. Improved interfacial bonding is attainable through fibre treatments such as chemical and physical procedures. The usefulness of the interface properties can be viewed within two aspects: first, it is responsible for good mechanical properties, and second it protects the composite properties from deterioration when submitted to environmental conditions, such as humidity. A weak interface allows fibre–matrix discontinuity by allowing the introduction of water between fibre and matrix through the interface, resulting in a loss of expected composite mechanical properties.

Micromechanical test methods have been used for the determination of the interface properties. The most used methods are the fragmentation test, the pull-out test and the micro-indentation test [1]. In this work, fragmentation tests were used to quantify the effect of chemical treatment (interfacial polycondensation at the surface of fibres) on glass fibres. The interfacial shear strength at the fibre–matrix interface was determined for treated and untreated fibre composites.

The single-fibre technique [2] has been used to determine interfacial shear strength as a measure of stress transferability of the interface. This method involves a single fibre totally encapsulated in a matrix. The matrix is stretched and the force is transferred to the fibre by a shear mechanism. The fibre breaks into small pieces until a critical length, l_c, is reached after which breakage stops. The shear stress, τ_e, at the fibre–matrix interface for a matrix that deforms plastically, with a perfect adhesion and a constant shear strength along the fibre length is given by

$$\tau_e = \frac{\sigma_f D_f}{2l_c} \quad (1)$$

where σ_f is the maximum stress experienced by the fibre at the critical length, D_f the fibre diameter, and, l_c the critical length of the fibres. Because fragment lengths are distributed between l_c and $l_c/2$, the mean fragment length, $\bar{l}_f$, which is derived from the experimentally observed fragment length is related to l_c by [3]

$$\bar{l}_f = 3/4\, l_c \quad (2)$$

The effective shear stress, τ_e, depends on the cumulative distribution of the fragment lengths. When combining Equations 1 and 2, τ_e can be expressed as

$$\tau_e = \frac{3\sigma_f D_f}{8\bar{l}_f} \quad (3)$$

To calculate $\bar{l}_f$ from the experimentally measured values of l, a distribution function has to be fitted to

† Author to whom all correspondence should be addressed.

0022–2461

the data. The most commonly used functions are Gaussian and Weibull distributions. The three-parameter Weibull distribution is given by [4]

$$p = 1 - \exp\left[-\left(\frac{l - l_u}{l_0}\right)^m \right] \quad (4)$$

where, in this case, p is the cumulative probability of failure, l the experimental values of the fibre fragment lengths, l_0 a scale parameter, m the parameter which simulates the shape of the curve and l_u the value below which the probability of failure is zero. If $l_u = 0$ as, for example, in the case of tensile stress of brittle materials [5], this equation simplifies to the two-parameter Weibull function. To calculate p, the following estimation is generally used [6]

$$p_i = \frac{i}{N + 1} \quad (5)$$

where i represents the order number of the fragment lengths when classified in an ascending order, and N the total number of fragments in the sample. To determine m, l_u and l_0, Equation 4 can be rewritten as follows

$$\ln(1 - p) = -\left(\frac{l - l_u}{l_0}\right)^m \quad (6)$$

and then

$$\ln\left[\ln\left(\frac{1}{1 - p}\right)\right] = m \ln(l - l_u) - m \ln l_0 \quad (7)$$

Therefore, the plot of $\ln[\ln(1/1 - p)]$ against $\ln(l - l_u)$ gives a straight line with a slope of m and l_u and l_0 can be determined by a least-square fitting method. Finally, the mean value of $\bar{l}$ is calculated as follows

$$\bar{l} = l_0 \Gamma(1 + 1/m) \quad (8)$$

where Γ is the gamma function. Alternatively, the value of $\bar{l}$ can be determined directly by fitting l and p to the Weibull function and extracting the value of $\bar{l}$ at $p = 0.5$.

2. Experimental procedure

2.1. Materials

Glass-fibre yarns with a diameter of 23 μm were supplied by Fiber Glass Canada. The fibres were washed with acetone in order to remove residual binder and organic impurities. Nylon-6,6 sheets of 15 cm × 15 cm × 0.75 mm used as the matrix, were supplied by Commercial Plastics (C.P.) Inc.

2.2. Polymer grafting on to the glass fibre surface

Solutions of 0.01 M hexamethylenediamine in water and of adipoyl chloride in dichloromethane were prepared. Long fibres (about 30 cm) were immersed first in the adipoyl chloride solution for 10 min, filtered and then immersed in the diamine solution. This procedure was repeated ten times in order to graft nylon-6,6 chains on to the fibre surface. The fibres were then washed with CH_2Cl_2 and water and vacuum dried at 110 °C for 24 h.

2.3. Sample preparation

Nylon-6,6 sheets were dried in a vacuum oven at 90 °C for 3 days prior to use. Single filaments of glass fibres were carefully extracted from chemically treated fibre bundles for each composite. Five single fibres were placed parallel to each other at a constant distance and held in place between two sheets of nylon. Two steel plaques covered by aluminium paper were used in the compression-moulding process, using a Carver Laboratory press at 285 °C. To prevent any physical damage to the fibres, the compression force was applied only when nylon began to melt. The mould pressure was then raised to 600 p.s.i. (10^3 p.s.i. = 6.89 N mm^{-2}) and maintained at that pressure for 5 min at 285 °C. Samples were then quenched by rapidly cooling the mould with water. This process was also repeated with untreated glass fibres. Samples were cut using a dumb-bell shaped mould according to ASTM D638 with fibre position parallel to the middle of the mould shape.

2.4. Tensile strength at mean fragment length

To measure the tensile strengths of the fibres at the mean fragment length, single-fibre tensile strength distributions were measured at different gauge lengths. Each monofilament was glued with a cyanoacrylate glue on a frame of a millimetric paper having a hole in the centre with a span equal to the desired gauge length. Tensile strengths were measured using a cross-head load of 500 g and a speed of 0.05 cm min^{-1}. For each gauge length, the tensile strength of 18–20 samples, each containing one monofilament, was determined.

2.5. Polarizing optical microscopy

Two single, treated and untreated glass fibres were placed each between two thin films of nylon-6,6 and were heated together between two glass microscope slides on a Mettler FP-80 hot stage at a heating rate of 20 °C min^{-1}. Nylon began to melt near 225 °C and the temperature was increased to 285 °C to remove all traces of crystallinity. The sample was cooled rapidly to 160 °C, maintained at this temperature for about 5 min and finally cooled down rapidly by a nitrogen stream until ambient temperature was reached. Samples were observed using a Zeiss polarizing optical microscope. The fibre diameter, D_f, was also measured using the microscope, and a value of 21 μm was measured and used in subsequent calculations.

2.6. Scanning electron microscopy

Fractured surfaces of the microcomposites after the failure of the samples in the tensile tests were analysed using a Jeol JSM-840 scanning electron microscope.

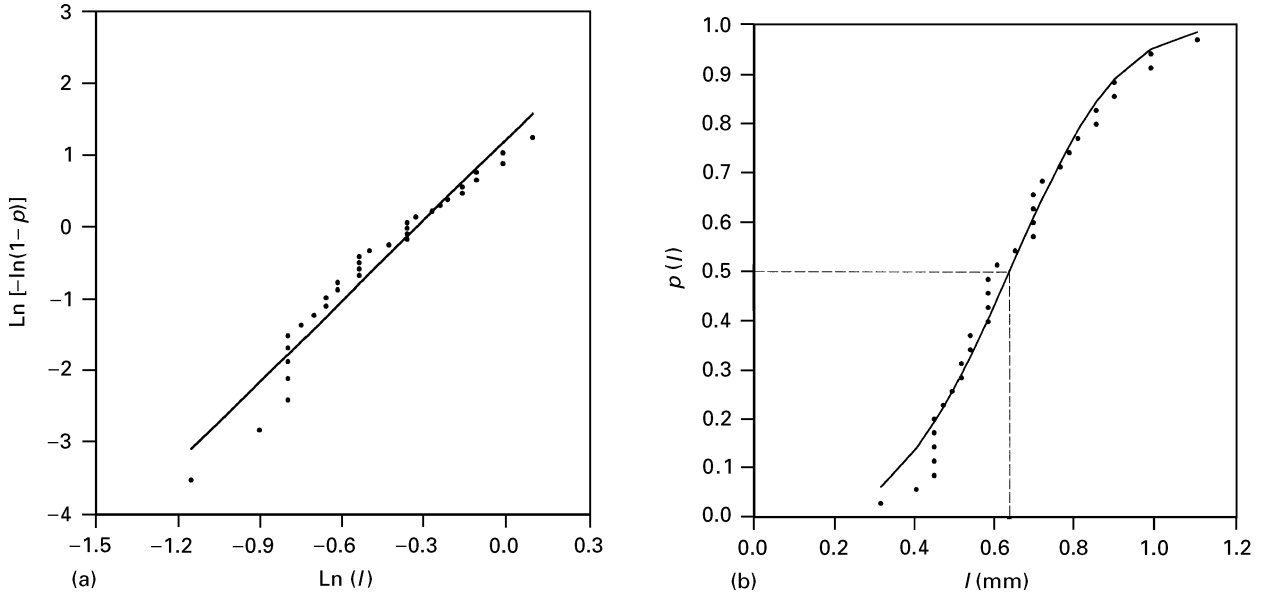

Figure 1 Determination of statistical distribution of fractured length for untreated fibre (a) Typical plot of $\ln[-\ln(1-p)]$ against $\ln(l)$, and (b) Weibull cumulative distribution of fragment lengths.

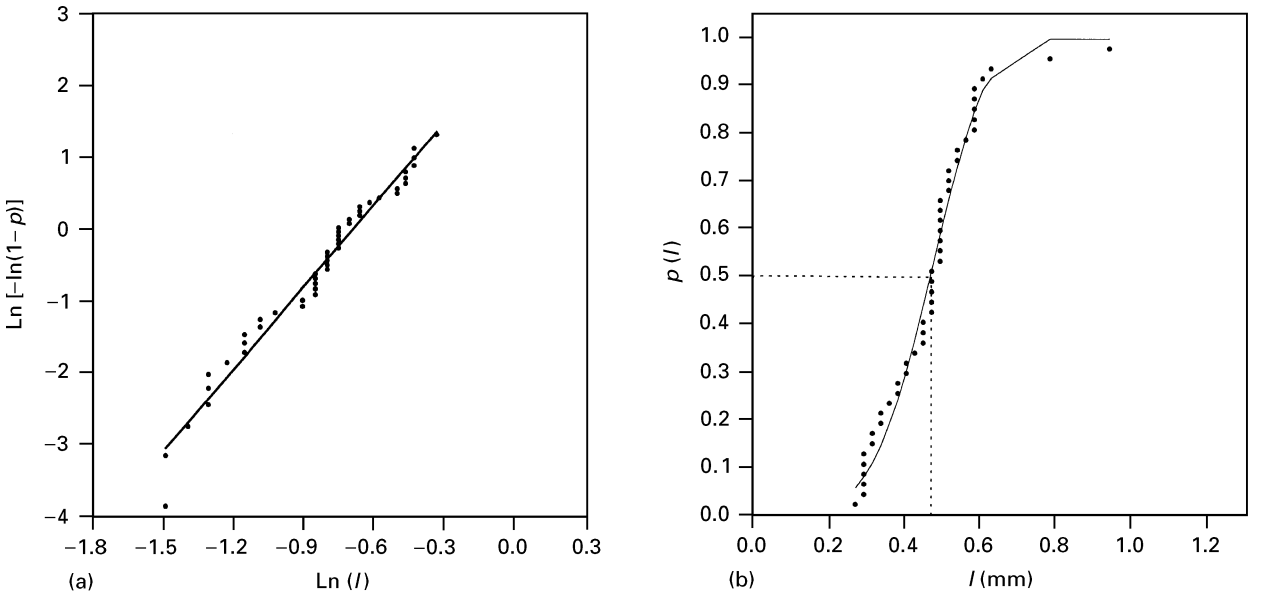

Figure 2 Determination of statistical distribution of fractured length for treated fibre (a) Typical plot of $\ln[-\ln(1-p)]$ against $\ln(l)$, and (b) Weibull cumulative distribution of fragment lengths.

A gold palladium alloy was cast on the fractured surface prior to investigation.

2.7. Sample fragmentation process

Samples were divided into two groups. The first group of samples was placed into a desiccator ("dry specimens") before experiments while the second group was stored in open air ("wet specimens") before carrying out fragmentation tests. For the first group ("dry specimens"), the samples were subjected to the tensile stress up to 10% strain using an Instron universal test machine with a force cell of 50 kgf (490.5 N) and a crosshead speed of 0.05 cm min^{-1} (8.33×10^{-6} m s^{-1}). The second series of specimens ("wet specimens") were pulled using different tensile stresses up to the breakage of the matrix. The fibre fragment lengths were observed and measured with the aid of a Zeiss optical microscope equipped with an eyepiece micrometer having a precision of 0.0225 mm.

A two-parameter Weibull distribution was examined in order to verify how well this distribution function can represent the experimental results. Figs 1a and 2a show typical diagrams of $\ln[-\ln(1-p)]$ versus $\ln(l)$ for fragmentation tests of untreated and treated samples which had been pulled to 10% strain. As can be seen, straight lines are obtained, which indicate that the two-parameter Weibull function is valid. The slope yields the Weibull shape parameter m, which is then used to calculate l_0. The correlation coefficients, r^2, determined by least squares when linear fitting was performed, are given in Tables I and II.

Once the Weibull parameters were found, the Weibull cumulative distributions of the fibre fragment

TABLE I Comparison of results using Weibull linear fitting and cumulative distribution, Gaussian distribution and arithmetic mean calculations for samples submitted to 10% strain

sample	m	l_0 (mm)	r^2	l_W (mm)	l_{Gauss} (mm)	l_{arith} (mm)
T_1	4.07	0.52	0.92	0.46	0.47	0.47
T_2	3.82	0.5	0.97	0.45	0.45	0.45
T_3	4.42	0.44	0.91	0.4	0.39	0.4
N_1	5.22	0.69	0.94	0.63	0.63	0.65
N_2	3.88	0.72	0.96	0.64	0.65	0.65
N_3	3.75	0.72	0.95	0.65	0.65	0.65

TABLE II Weibull linear fitting and cumulative distribution, Gaussian distribution and arithmetic mean calculations for samples submitted to different strains

sample	m	l_0 (mm)	r^2	l_W (mm)	l_{Gauss} (mm)	l_{arith} (mm)
T_4	3.45	0.75	0.97	0.67	0.67	0.67
T_5	2.7	0.83	0.93	0.73	0.74	0.73
T_6	3.47	0.52	0.95	0.46	0.47	0.47
T_7	4.09	0.57	0.86	0.51	0.51	0.51
T_8	3.77	0.55	0.93	0.49	0.48	0.49
N_4	4.15	0.72	0.94	0.65	0.65	0.65
N_5	4.15	0.72	0.94	0.64	0.65	0.65
N_6	3.33	0.9	0.97	0.81	0.8	0.8
N_7	3.23	0.77	0.96	0.67	0.68	0.69
N_8	3.51	0.74	0.93	0.66	0.66	0.66

lengths were fitted to the experimental values using Equation 9

$$P(l) = 1 - \exp[-(l/l_0)^m] \quad (9)$$

The cumulative probability, $P(l)$, in Equation 9 for each sample group is depicted in Figs 1b and 2b. From these fittings, the values of $\bar{l}$ at $P(l) = 0.5$ was obtained. This value is equal to the mean fragment length ($\bar{l}_f$).

3. Results and discussion

3.1. Analysis of the fragment lengths

In order to evaluate the results better, in addition to Weibull distributions, Gaussian distributions were also used to analyse the experimental data. A simple arithmetic mean of fragment lengths, l_{arith}, was also calculated for each sample. Table I shows the results of the Weibull linear fitting and cumulative distribution, as well as the Gaussian distributions for the samples pulled up to 10% strain. Mean fragment lengths obtained from Weibull, Gaussian and arithmetic calculations are presented as l_w, l_{Gauss} and l_{arith}, respectively. Table II presents the results of samples which have been submitted to different strains and stresses. Tensile strengths of the fibres at mean fragment lengths were obtained from the plot of $\ln \sigma_f$ versus $\ln(l_g)$, l_g being the gauge length, and are reported in Fig. 3. Four different gauge lengths were used and a linear fitting was performed by a simple least squares method. The resulting r^2 of 0.94 indicates a good fit. Once the values of σ_f were determined, τ_e was calculated using Equation 3.

When comparing the results of Gaussian and Weibull distributions, similar values for $\bar{l}$ are obtained.

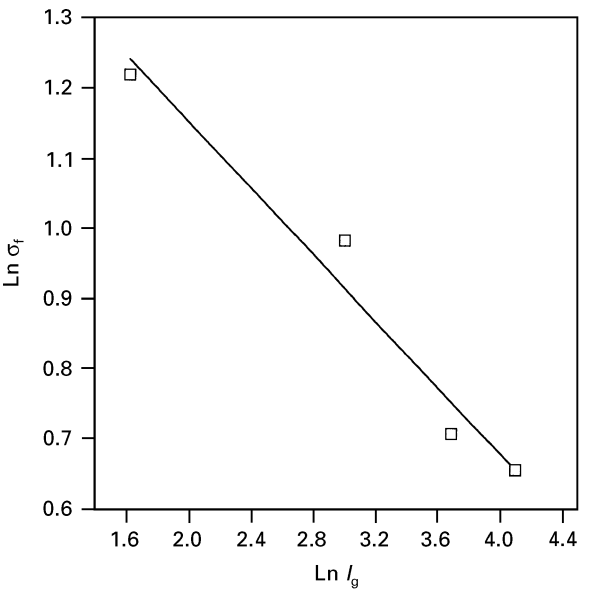

Figure 3 Variation of mean tensile strengths of single fibres with respect to gauge lengths.

It is concluded that, for a system of glass fibres embedded in a nylon-6,6 matrix, these two distribution functions can be used to fit the experimental results. Moreover, when comparing these data with those of simple arithmetic means of fragment lengths, similar values are also found for $\bar{l}$. The same phenomenon has been reported in a study on carbon fibres [6]. The agreement between the three methods used in determining $\bar{l}$ indicates that the number of samples used in this study is large enough to ensure statistically meaningful results.

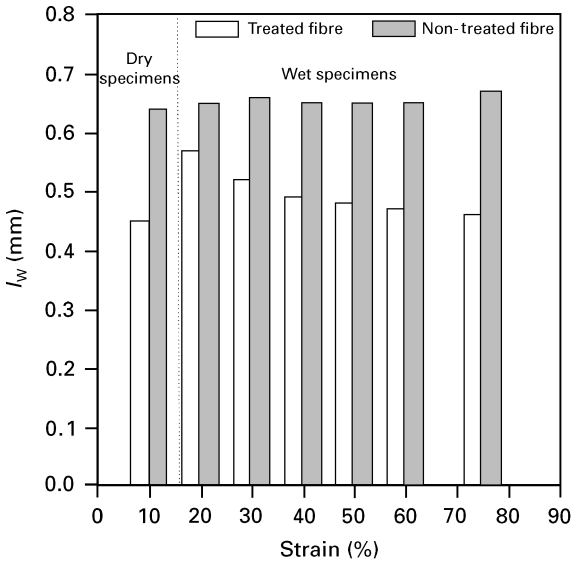

Figure 4 Variation of fibre mean fragment lengths of dry and wet specimens with strain.

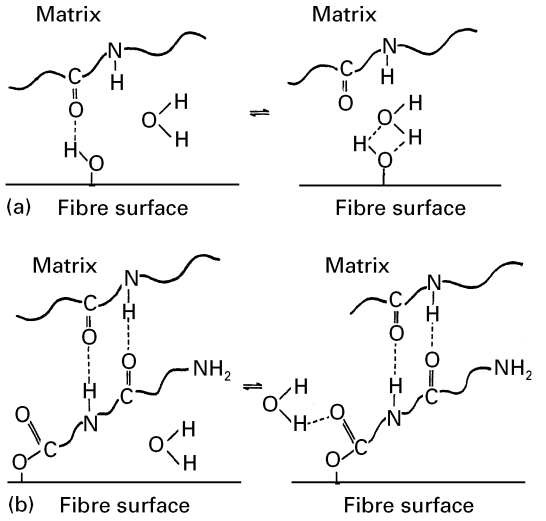

Figure 5 Schematic representation of the effect of the humidity on the fibre–matrix interface: (a) untreated fibre; (b) treated fibre.

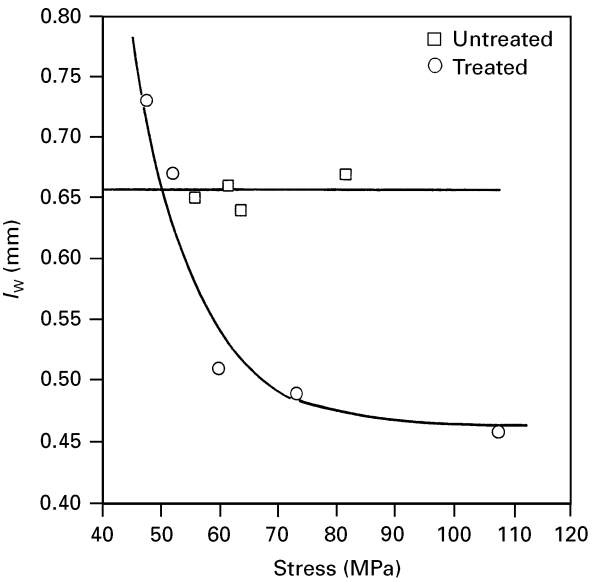

Figure 6 Variation of fibre mean fragment lengths with stress for (□) untreated and (○) treated fibre.

3.2. Effect of grafted molecules on the interfacial shear strength

Fig. 4 shows the mean fragment lengths of dry and wet specimens. As mentioned earlier, dry specimens were submitted to 10% strain and wet specimens were submitted to different strains. The results obtained from the fragmentation tests of dry samples indicated that an important change in the fibre–matrix adhesion was achieved. It can be seen readily from this figure that the mean fragment lengths are reduced by 30% as compared to untreated samples. Using these values to calculate the effective interfacial shear stress gives an increase of τ_e up to 59% due to the chemical treatment of the glass fibres.

As mentioned earlier, the presence of a good interface is also essential to the retention of the composite mechanical properties in a real environment in which humidity and other factors affect composites. In order to evaluate this effect, a second group of samples was placed in open air in 50% humidity for 2 weeks and the results are presented in Table II.

3.3. Effect of humidity on the interface quality

When comparing the l_w values with those of dry samples, an increase is observed when samples are allowed to absorb water from the atmosphere for both treated and untreated samples. Water weakens hydrogen bonds in nylon-6,6, which results in matrix plastification, and an observed lowering of τ_e. It is therefore not possible to compare the results at 10% strain for dry and humid systems because the matrix properties are changed. It is, however, reasonable to compare the evolution of the interface with the applied strain, as illustrated in Fig. 4. A continuous decrease of l_w is observed with increasing strain for the treated fibres while, in the case of untreated fibres, l_w remains almost unchanged. When comparing l_w, it can be found that, for a given strain, the value of l_w is much lower for the treated fibres. This is related to the efficiency of the interface to transfer the strain to the fibre, which induces fibre breakage when exceeding the maximum breaking strain of the fibre. The humidity affects τ_e by two mechanisms; first, it causes a matrix strength loss, and second, it directly affects the fibre–matrix interface. Water is proposed to compete in the formation of hydrogen bonds with OH groups of the glass fibres. This competition weakens matrix–fibre hydrogen bonds. However, for treated samples, fibre–matrix interactions are composed of both covalent bonds and hydrogen bonds. The effect of humidity will therefore be mainly the plastification of the matrix, while the interface will remain relatively unaffected. This phenomenon is illustrated in Fig. 5.

Fig. 6 presents the variation of the mean fragment lengths of both treated and untreated fibres with stress. For untreated samples, l_w does not vary significantly with stress. In the case of treated samples, the behaviour is completely different. A sharp decrease is first observed upon increasing the stress and then the

mean fragment length tends asymptotically towards a constant value for higher stresses. The results of Fig. 6 give an average asymptotic value of 0.48 mm for l_w. The corresponding τ_e, calculated using Equation 3, is 99.4 MPa. The maximum shear stress of the matrix has been reported as being 66.2 MPa [7] and the τ_e value calculated using Fig. 6 is therefore considerably higher than that of the matrix. Moreover, humidity could effectively contribute to an underestimation of this value by reducing maximum shear stress of the matrix.

Higher values of τ_e are related to the difference in shear properties of the bulk matrix and of the interphase [8]. For untreated fibres, a value of 0.65 mm for l_w is obtained, which corresponds to a τ_e value of 68.4 MPa. This value is, as expected, much lower than that of treated fibres and very close to that of the pure matrix. As mentioned previously, when a single fibre embedded in a matrix is stretched, the force is transmitted to the fibre by a shear mechanism and the fibre breaks into small pieces. The length of these pieces becomes shorter with increasing stretching through additional breaking of the fibre. This will happen only when the fibre–matrix adhesion is such that the load transfer from the matrix to the fibre is allowed. Lack of fibre–matrix adhesion causes the matrix to slip around the fibre without fibre breakage. This phenomenon was observed, for example, when a liquid crystalline fibre was embedded in a polycarbonate matrix [9]. As seen in Fig. 6, l_w does not vary when stress increases for untreated samples. This indicates that the force applied to the matrix was not transmitted to the fibre through the interface and thus, that no further breakage occurred when the force was increased. It is concluded that the fibre–matrix adhesion was weak when untreated fibres were used.

Further evidence can be derived when comparing applied stress on the samples. From Fig. 6, it can be seen that the stress corresponding to the minimum fragment length (0.64 mm) for untreated fibres is 63.2 MPa. For the same value of l_w for treated samples, a stress of 52 MPa is obtained, a value considerably lower. This means that, in the case of treated samples, the fibres carry the applied load transmitted from the matrix through the interface. This is the favourable condition expected for composites. For untreated samples, it is essentially the matrix which supports the load. Therefore, it can be concluded that for continuous fibre composites, early failure of the matrix will cause the failure of composite. This again confirms the efficiency of the interface to transfer the load from the matrix to the fibre in treated fibres.

Possible explanations for obtaining higher τ_e could be that, in the case of treated samples, properties of the matrix layer which lies at the interface are quite different from those of the bulk matrix. The ability of the fibre to induce transcrystallinity has to be taken into account, because the properties of the transcrystalline layer are known to be different from those of the neat resin [10]. This ability could be due to chemical affinity between the fibre surface and the matrix, which also could cause the transcrystalline layer observed by optical polarizing microscopy of the fibres subjected to surface treatment [11]. In order to analyse the fibre surface evolution during the grafting procedure, the fibres were observed through a scanning electron microscope (SEM). Scanning electron micrographs of the single fibres are given in Fig. 7. Fig. 7a shows the surface of acetone-washed glass fibre and Fig. 7b illustrates a glass-fibre surface which has been submitted to the polymer grafting reaction. Nylon-6,6 deposits are clearly observed. However, these are not distributed evenly on the fibres, which may indicate the presence of non-grafted polymer. Washing with trifluoroethanol was performed in order to remove this fraction. This solvent was chosen for its ability to dissolve nylon-6,6 while having a low acidity. The use of an acidic solvent such as trifluoroacetic acid, *m*-cresol or sulphuric acid, which are all good solvents for nylon-6,6, would undoubtedly have hydrolysed O–C=O bonds created at the interface. Even with trifluoroethanol, some hydrolysis may have occurred. Fig. 7c shows the surface of a grafted fibre after washing with trifluoroethanol. Remaining structures are identified as the grafted polymer. These could act as a nucleating surface and be responsible for enhanced transcrystallinity.

Optical micrographs of the transcrystalline layer are illustrated in Fig. 8. There is no evidence of a continuous transcrystallinity in untreated samples while there is a clear transcrystalline interphase in the samples containing grafted glass fibres. It can be concluded that, when the conditions allow its growth, a transcrystalline layer can be formed around the treated fibres. Under the same conditions, no change was observed for untreated fibres. Because the aim of this work was not to study the effect of transcrystallinity on the fibre fragmentation test, samples were not prepared for this purpose. However, this observation is an additional indication on the effect of the treatment on fibre–matrix interface.

Further evidence of the effect of the fibre treatment is obtained through SEM analysis of the fracture surface of selected samples. Fig. 9 shows the interface regions of the samples after the failure of the microcomposites in the fragmentation test. It is obvious from these pictures that, for the untreated fibre, a hole has appeared in the matrix indicating that fibre pull-out has occurred (Fig. 9a). For the treated fibre composite, there is no hole formation and structural units of leftover fibre fragments and matrix are present instead. This indicates that the failure mechanism is primarily fibre failure, which in turn is related to an excellent adhesion (Fig. 9b). As mentioned earlier in this paper, in the former case, this type of fibre–matrix debonding results from poor adhesion between fibre and matrix, which allows the matrix to slip around the fibre without fibre failure. This can explain why, in the case of untreated fibres, the values of l_w are higher than those of treated fibres and why l_w does not change when applied stress and/or strain increases. However, good adhesion, as shown in Fig. 9b, is responsible for the load transfer from the matrix to the fibre, resulting in lower l_w values as well as a lowering of l_w when increasing the applied stress or strain. The resulting interface could be very different from the

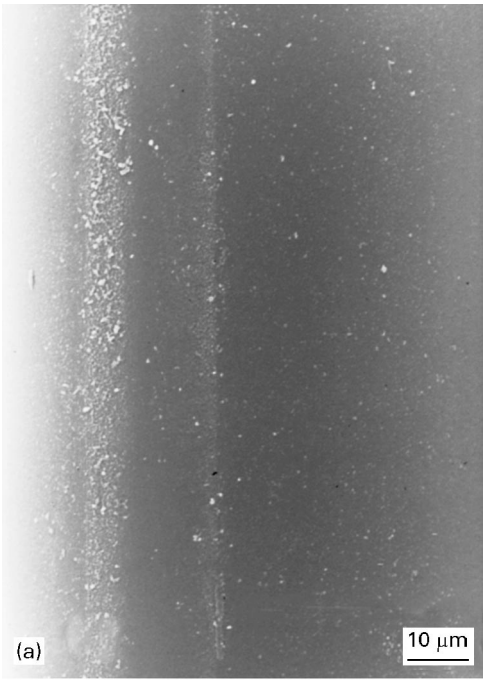

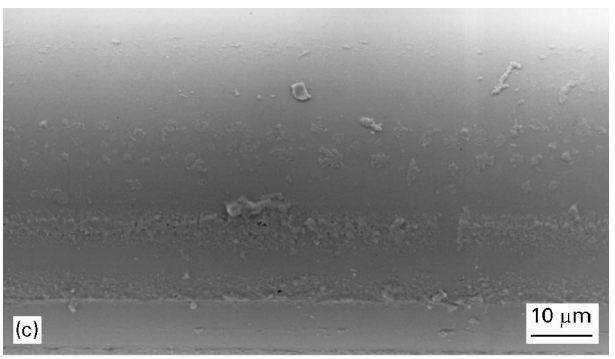

Figure 7 Scanning electron micrographs of the surface of glass fibres: (a) washed fibre, (b) grafted fibre; (c) grafted fibre washed with trifluoroethanol.

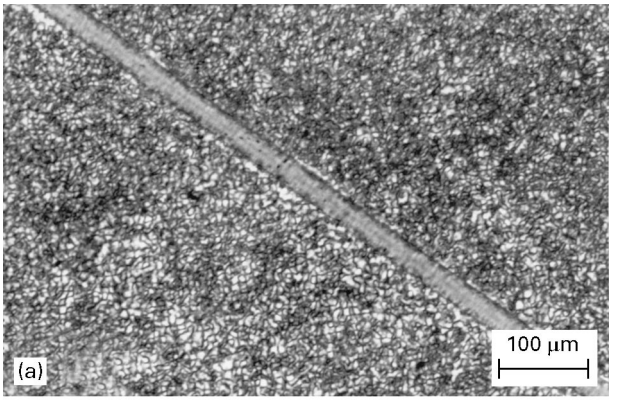

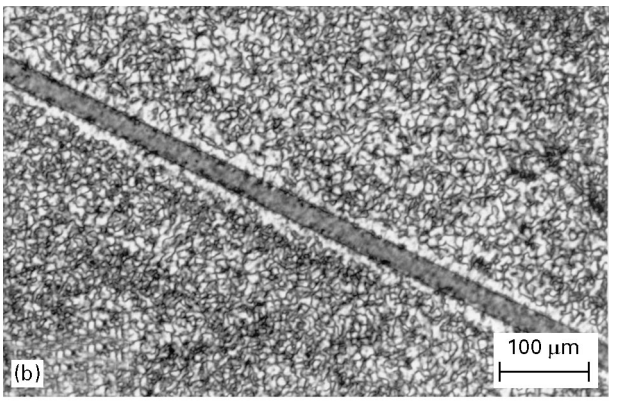

Figure 8 Optical micrographs of a single glass fibre embedded in nylon,6-6 matrix: (a) untreated fibre, (b) treated fibre.

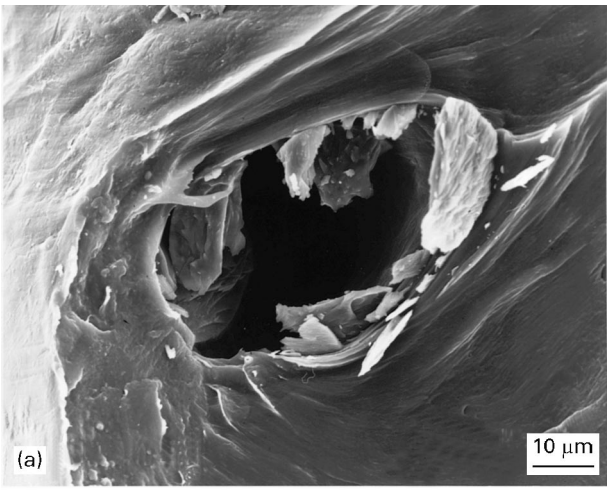

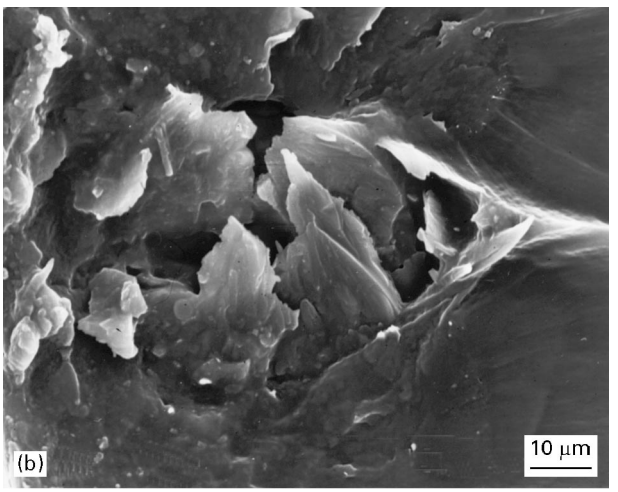

Figure 9 Scanning electron micrographs of fractured surface of microcomposites: (a) untreated fibre, (b) treated fibre.

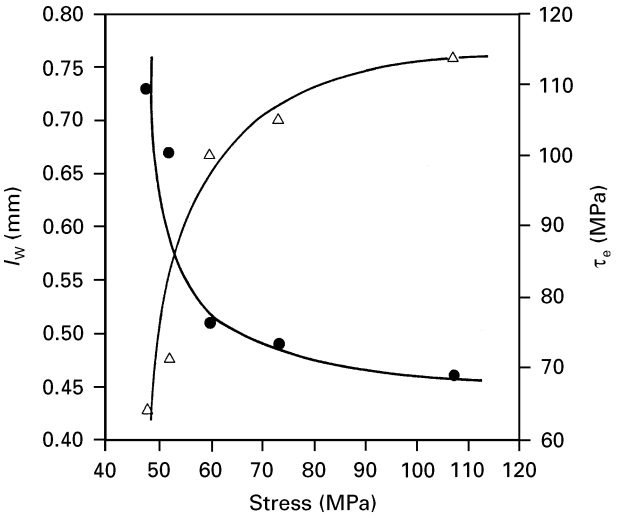

Figure 10 (△) Interfacial shear strength and (●) mean fragment length as a function of stress in treated fibres.

matrix itself, which could explain why interfacial shear strengths obtained in this study exceed those of the matrix. These observations are depicted in Fig. 10, in which the effects of applied stress or strain on the mean fragment lengths and resultant interfacial shear strengths of treated fibres, are demonstrated.

Another factor contributing to higher values of τ_e is the value of σ_f. In this study, tensile strength of the fibres at mean fragment length was determined using different gauge length measurements, as in a previous work [6]. Another possible way to calculate σ_f at short fibre lengths is to use the Weibull equations, assuming the Weibull parameters are known. This can be done only when the Weibull parameters are independent of gauge lengths. In this study, it was found that the Weibull parameters change with gauge length and therefore this approach has not been used to determine fibre strength at short lengths such as the mean fragment lengths.

4. Conclusions

Interfacial polymerization of nylon-6,6 on the surface of glass fibres was used to attach nylon chains to the fibre surface, which in turn changed fibre surface properties. Residual nylon-6,6 was observed at the glass fibre surface through SEM. The modification increased fibre–matrix adhesion, so that higher values of interfacial shear strengths were obtained with treated fibres. Fibre–matrix interface properties observed by SEM showed clear changes in the behaviour of the interface. The fracture mechanism changed from fibre pull-out, in the case of untreated fibre to fibre failure for treated samples, which clearly indicated a considerable increase in interface adhesion. Finally, it was shown that the two-parameter Weibull distribution can be applied to fibre fragment lengths in order to derive the values of mean fragment length used in the interfacial shear strength calculations.

Acknowledgements

The financial support of the Natural Sciences and Engineering Council of Canada (NSERC) and of the Fonds pour la Formation des Chercheurs (FCAR) of the province of Quebec is gratefully acknowledged. One of the authors benefited from a scholarship from the Ministry of Science and Higher Education of Iran.

References

1. I. VERPOEST, M. DESAEGER, J. IVENS and M. WEVERS, *Makromol. Chem. Macromol. Symp.* **75** (1993) 85.
2. A. KELLY and W. R. TYSON, *J. Mech. Phys. Solids* **13** (1985) 329.
3. A. S. WIMOLKIATISAK and J. BELL, *Polym. Compos.* **10** (1989) 162.
4. W. WEIBULL, *J. Appl. Mech.* **18** (1951) 293.
5. K. TRUSTRUM and A. DE. S. JAKATILAKA, *J. Mater. Sci.* **14** (1979) 1080.
6. EL. M. ASLOUN, J. B. DONNET, G. GUILPAIN, M. NARDIN and L. SCHULTZ, *ibid.* **24** (1989) 3504.
7. J. BRANDRUP and E. H. IMMERGUT, "Polymer Handbook" (Interscience, New York, 1966).
8. A. S. WIMOLKIATISAK and J. BELL, *Polym. Compos.* **10** (1989) 162.
9. C. CARFAGNA and P. A. NICOLAIS, *ibid.* **13** (1992) 169.
10. B. S. HSIAO and E. J. H. CHEN, "Controlled Interphase in Composite Materials", edited by H. Ishida (Elsevier Science, New York, 1990) p. 613.
11. H. SALEHI MOBARAKEH, A. AIT-KADI, J. BRISSON, *Polym. Eng. Sci.*, **36** (1996) 778.

Received 10 August 1995
and accepted 13 June 1996